



Universiteit
Leiden
The Netherlands

Targeting TGF β signaling pathway in fibrosis and cancer

Karkampouna, S.

Citation

Karkampouna, S. (2016, January 28). *Targeting TGF β signaling pathway in fibrosis and cancer*. Retrieved from <https://hdl.handle.net/1887/37560>

Version: Corrected Publisher's Version

License: [Licence agreement concerning inclusion of doctoral thesis in the Institutional Repository of the University of Leiden](#)

Downloaded from: <https://hdl.handle.net/1887/37560>

Note: To cite this publication please use the final published version (if applicable).

Cover Page



Universiteit Leiden

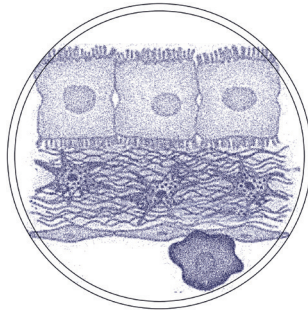


The handle <http://hdl.handle.net/1887/37560> holds various files of this Leiden University dissertation.

Author: Karkampouna, Sofia

Title: Targeting TGF β signaling pathway in fibrosis and cancer

Issue Date: 2016-01-28



Chapter 3

Inhibition of TGF β type I receptor activity facilitates liver regeneration upon acute CCl₄ – intoxication in mice

Sofia Karkampouna¹, Marie-José Goumans¹, Peter ten Dijke¹, Steven Dooley² and Marianna Kruithof-de Julio^{1,3,*}

¹Department of Molecular and Cell Biology, Centre of Biomedical Genetics, Leiden University Medical Center, Leiden, The Netherlands

²Molecular Hepatology - Alcohol Associated Diseases II Medical Clinic Medical Faculty Mannheim, Heidelberg University, Mannheim, Germany

³Department of Dermatology, Leiden University Medical Center, Leiden, The Netherlands

* Corresponding author

Archives of Toxicology, 2015 Jan 8. PMID: 25566828

Abstract

Liver exhibits a remarkable maintenance of functional homeostasis in presence of a variety of damaging toxic factors. Tissue regeneration involves cell replenishment and extracellular matrix remodeling. Key regulator of homeostasis is the transforming growth factor-β (TGFβ) cytokine. To understand the role of TGFβ during liver regeneration, we used the single-dose carbon tetrachloride (CCl₄) treatment in mice as a model of acute liver damage. We combined this with *in vivo* inhibition of the TGFβ pathway by a small molecule inhibitor; LY364947, which targets the TGFβ type I receptor kinase (ALK5) in hepatocytes but not in activated stellate cells. Co-administration of LY364947 inhibitor and CCl₄ toxic agent resulted in enhanced liver regeneration; cell proliferation (measured by PCNA, phosphorylated histone 3, p21) levels were increased in CCl₄+LY364947 versus CCl₄-treated mice. Recovery of CCl₄-metabolizing enzyme CYP2E1 expression in hepatocytes is enhanced seven days after CCl₄ intoxication in the mice that received also the TGFβ inhibitor. In summary, a small molecule inhibitor that blocks ALK5 downstream signaling and halts the cytostatic role of TGFβ pathway results in increased cell regeneration and improved liver function during acute liver damage. Thus, *in vivo* ALK5 modulation offers insight into the role of TGFβ, not only in matrix remodeling and fibrosis, but also in cell regeneration.

Keywords

Acute-Hepatotoxicity- CCl₄- Regeneration- ALK5- LY364947- TGFβ- Smad

Introduction

Liver tissue has high regenerative capacity in response to damaging stimuli such as virus infections, chemicals, and alcohol intoxication^{1,2}. Liver regeneration involves replenishment of dead epithelial and mesenchymal cells by proliferation and restoration of normal tissue architecture by fibrous scar formation³. Chronic organ damage leads to exhaustion of the cell pool and fibrosis, excess accumulation of extracellular matrix proteins (ECM) and eventually to clinical complications such as acute liver failure⁴. Thus, there is a need for better understanding of the mechanisms regulating innate tissue regeneration.

Application of the hepatotoxin carbon tetrachloride (CCl₄) is an established experimental animal model for liver regeneration since single administration of CCl₄ *in vivo* leads to acute and reversible liver damage⁵. Liver regeneration occurs within 7-8 days without affecting any other organ system. Only a specific subset of hepatocytes, located around the central veins, appears to be damaged due to unique expression of CCl₄-metabolising enzyme Cytochrome 450 (Cyp2E1)^{3,6}. In turn, cytokines and stress signals derived from hepatocytes induce the activation of hepatic stellate cells (HSCs) into myofibroblasts (MFBs). The αSMA expressing MFBs⁷ appear in clusters around the central vein and assist tissue repair by scar ECM formation. Simultaneously, quiescent HSCs located in the space of Disse become activated by cytokines released from damaged hepatocytes, and concentrate in the central vein area, e.g. due to migration and/or proliferation.

Transforming growth factor-β (TGFβ) signaling plays an important role in maintenance of liver homeostasis, terminal differentiation and apoptosis of hepatocytes⁸. Under liver damage conditions, TGFβ1 is up regulated and regulates parenchymal, inflammatory cells and HSCs^{6,9,10}. Although many cells in the liver may produce TGFβ1, Kupffer cells and recruited

macrophages are the major source of TGF β . TGF β 1 is critical for activation of HSCs into MFBs, stimulates ECM production and inhibits ECM degradation¹⁷. Activated HSCs, and to lesser extent, sinusoidal endothelial cells (ECs), also contribute to increased TGF β production⁴. However, TGF β in the liver has additional actions, such as immunomodulatory properties and its cytostatic effects on epithelial cells (hepatocytes)¹². The regenerative capacity of the liver is characterised by hepatocyte proliferation but also by increased TGF- β 1 expression¹³. The level of DNA synthesis is maximal during the first 48 hours after CCl₄ intoxication, coinciding with the TGF β increase in the liver^{6,14}. Thus, hepatocytes proliferate despite the presence of an antiproliferative stimulus; however, the exact mechanism of this process is unclear. Administration of TGF β *in vivo* after partial hepatectomy reduces the number of hepatocytes that progress from G1 to the DNA synthesis phase¹⁵. It has been proposed that during early response after liver injury, hepatocytes become transiently resistant to TGF β either by down regulation of TGF β receptors¹⁴ and TGF α protective action¹⁵ or by up regulation of transcriptional repressors¹⁶. Levels of T β RI and T β RII mRNA expression in rat hepatocytes decreased from 12 to 48 hours and returned to normal by 72 hours after CCl₄ administration, while T β RI and T β RII mRNA were expressed constantly in non-parenchymal cells¹⁴. Thus, the function of TGF β is cell-type specific and its role on liver regeneration remains largely unknown.

TGF β is synthesized and stored in the ECM as a latent complex with its prodomain, LAP (latency-associated peptide). Latent TGF β is considered to be a molecular sensor that responds to specific signals by releasing active TGF β ¹⁷. These signals are often perturbations of the ECM that are associated with angiogenesis, wound repair, inflammation and, perhaps, cell growth¹⁸. Changes in the cell's environment are relayed to the sensor by a number of different molecules, including proteases, integrins and thrombospondin¹⁹. TGF β functions by binding to cell surface receptors. Binding of free TGF β ligands to its type II receptor causes the activation of the type I receptor, ALK5 and the assembly of a protein complex which further phosphorylates and activates the R-Smads, Smad2 and Smad3. Subsequent signal transduction occurs when the active Smad2 and Smad3 transcription factors form complexes with Smad4, and translocate from the cytoplasm to the nucleus²⁰ to induce TGF β target gene expression.

Several studies have investigated the therapeutic potential of inhibition of TGF β in lung, kidney and liver diseases and a number of compounds have reached the phase of clinical trials²¹. Smad3-deficient mice develop reduced dermal²², renal²³ and liver fibrosis²⁴. However, the complexity of the TGF β pathway, its involvement in a plethora of cellular processes and cell type specific effects impede the design of therapies in the context of liver diseases. For instance, loss of TGF β signaling in fibroblasts causes intraepithelial neoplasia, suggesting that TGF β controls the activity of fibroblasts as well as the oncogenic potential of neighbouring epithelial cells²⁵. Experimental regeneration models such as partial hepatectomy indicate a role for TGF β only at late stage of wound healing, mainly for restoration of ECM and new vessel formation⁷. The pleiotropic effects of TGF β upon different cell types (hepatocytes and HSCs) and the time of action during liver damaging conditions remain yet unclear.

To study the mechanisms behind liver regeneration in regards to TGF β signaling, in a time-dependent manner, we have selected the CCl₄-induced acute liver damage model. A single dose of CCl₄ leads to reversible centrilobular necrosis and steatosis²⁶, while prolonged administration leads to liver fibrosis, cirrhosis, and hepatocellular carcinoma. CCl₄ impairs hepatocytes directly by altering the permeability of plasma, lysosomal, and mitochondrial membranes²⁷. We investigated the effects of *in vivo* inhibition of the TGF β receptor by the

small molecule inhibitor LY364947 (LY) during CCl₄-induced acute liver injury in order to delineate its function on hepatocytes and HSCs. LY is an ATP-competitive, cell permeable inhibitor, selective for TGFβ type I Activin receptor-like kinases (ALK4, 5 and 7)²⁸. In this study we show that, regarding *in vivo* TGFβ inhibition, the LY compound seems to be effective in epithelial cells, particularly centrizonal hepatocytes, and enhances their proliferation and regeneration in CCl₄- acute injury model.

Materials and Methods

Acute liver damage model and administration of small molecule inhibitors

Animal protocols were in full compliance with the guidelines for animal care and were approved by the Leiden University Medical Center Animal Care Committee. Acute liver injury was induced in 5-6 weeks old male C57Bl6 mice weighing 20 - 25 g by intraperitoneally injecting a single dose of 1 ml/kg body weight CCl₄ (mixed 1:1 with mineral oil), and mice were sacrificed after days 1, 2, 3, and 7 (n=2 per time point). LY364947 (5 mg/kg, Axon Medchem) was intraperitoneally injected 1 hour prior to CCl₄ shot on day 0. Every 24 hours since the first injection, the compound was administered (day 0- day 3). From day 3 to day 7 mice did not receive any compounds and were sacrificed after days 1, 2, 3, and 7 (n=3 mice per group and per time point). Control group received DMSO (1mg/kg mixed with PBS), LY364947 (5 mg/kg) received 4 injections every 24 hours. During day 3 to day 7, mice did not receive LY364947 and were sacrificed after days 1, 2, 3, and 7 (n=2 mice per group and per time point). From the liver tissues collected, one lobule was used for histology preparation, one lobule for RNA isolation and one lobule for protein isolation per individual mouse.

More information on Supplementary Materials and Methods.

Results

Phenotypic changes in acute CCl₄-induced liver damage model

Induction of liver damage was performed by single injection of hepatotoxic agent CCl₄ in 5-6 week old male C57Bl6 mice. At several time points after vehicle control or CCl₄ injection (day 1, day 2, day 3, day 7) mice were sacrificed and liver tissue was collected. Upon liver damage, hepatocytes located around the central vein area metabolize CCl₄ and undergo functional and phenotypic changes, such as loss of hepatocyte marker HNF4α (**Fig.1A**). Dormant HSCs are distinguished by desmin expression and lack of αSMA staining, the latter being up regulated only upon activation of HSCs (**Fig.1A**). Highest expression of αSMA is reached during day 3 (**Fig.1A**) after single CCl₄ injection. Increased collagen staining in the CCl₄-injected livers (**Fig.1A**) represents the cell population of activated HSCs, which produce ECM proteins such as collagen type I and fibronectin. During mouse liver homeostasis, TGFβ is active, as nuclear phosphorylated Smad2 (pSmad2) protein is seen in hepatocytes of normal liver (**Fig.1B**) at various time points after injection with vehicle compound (day1, day2, day3, day7). Upon tissue damage active TGFβ ligands are released leading to activation of profibrotic gene expression and wound healing response in the activated HSCs. We have observed that pSmad2 nuclear localization follows a specific spatiotemporal pattern in the hepatocytes during the early time points after acute injury. Immunostainings for HNF4α,

pSmad2 and α SMA (**Fig.1A-B**) indicate that damaged hepatocytes adjacent to the central vein area transiently down regulate expression of HNF4 α (**Fig.1A**) and pSmad2 (**Fig.1B**), almost immediately upon tissue damage. In turn, α SMA+ HSCs accumulate in the central vein between day 2- day 3 and activate pSmad2 (**Fig.1B**). This effect is transient, since pSmad2 expression is restored in the regenerated hepatocytes after seven days (**Fig.1B**). The distribution of HSCs at seven days after CCl₄ shot is similar to the control liver tissue (**Fig.1B**).

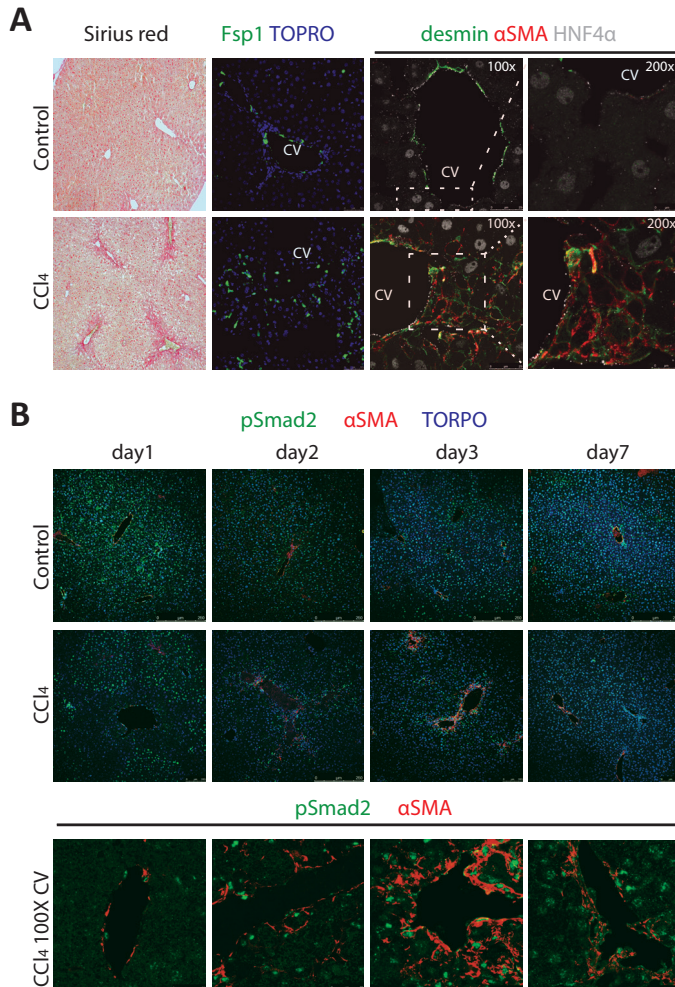


Fig.1. Acute CCl₄-induced liver damage model

(A). From left to right: Picosirius red staining for visualization of collagen fibers in liver tissues of control and CCl₄-treated mice (magnification: 10x). Immunofluorescence staining indicates protein expression of Kupffer cell marker; Fsp1 (magnification: 40x, scale bars=50 μ m). HSC markers; desmin (green) and α SMA (red), hepatocyte-specific marker HNF4 α (grey) in control and CCl₄-injected liver tissues (magnification: 100x, scale bars=250 μ m). The marked area is shown at higher magnification (200x), scale bars= 10 μ m. Nuclei (blue) were visualized by TOPRO-3 nuclear dye. Damaged central vein area is distinguished by expression of α SMA-positive HSCs (red) and loss of hepatocyte marker HNF4 α (grey). Time point: day 3 (72 hours after CCl₄). (B). Time course of pSmad2 (green) and α SMA (red) co-localisation by immunofluorescence during acute liver damage. Representative images of liver tissues from vehicle and CCl₄- injected mice are shown (magnification: 20x. Scale bars=100, 250 μ m). Bottom panel: image of higher magnification of the central vein (CV) (CCl₄, 100x CV). Scale bars= 25 μ m. Time course (1, 2, 3, 7 days).

Effects of ALK5 inhibitor (LY) on TGF β signaling and hepatic apoptosis *in vivo*

In order to interfere *in vivo* with TGF β signaling activation we have used the small molecule inhibitor (LY364947), which selectively blocks kinase activity of ALK5. The LY compound was injected one hour prior to CCl₄ administration, in order to inhibit the TGF β pathway shortly before the induction of cellular damage (**Fig.2A**). Administration of the compound was performed every 24 hours for 4 days (day 0- day 3) in mice that also received a single shot of CCl₄ or vehicle control at day 0 (**Fig.2A**). Mice injected with vehicle substance or LY compound have normal liver morphology (**Fig.S1**). Early response (24 hours) to tissue damage involves transient loss of nuclear phosphorylated Smads (pSmad2) specifically in damaged hepatocytes of the central vein area (**Fig.2B**). To further test this observation, pSmad2 protein levels were measured in whole liver homogenates in control (vehicle), CCl₄ and CCl₄+LY-treated mice (**Fig.S2**). In addition, reduced pSmad2 immunofluorescence staining is observed in livers that were treated only with LY (**Fig.S1**), suggesting that the LY inhibitor can attenuate the activation of ALK5/Smad2 pathway in hepatocytes. Time course of pSmad2 immunofluorescence in the damaged (CCl₄) liver tissues, indicates further inhibition of pSmad2 signal after treatment with the inhibitor (**Fig.2B**). However, co-labeling of α SMA and pSmad2 (**Fig.2B**; **Fig.S3**) shows that HSCs still have active pSmad2 and may not be efficiently targeted by LY inhibitor when administered systemically. Hepatic mRNA expression of p21, enriched in hepatocyte population and TGF β target gene, is down regulated after LY administration (**Fig.2C**); however expression of Collagen type I (Col1A1), that is enriched in the HSC population, is not effectively inhibited but even induced by the LY (**Fig.2D**). In addition, inhibitory role of LY on mRNA expression of Plasminogen activator type 1 (Pai-1) in whole liver extracts, is observed only at 48 hours after CCl₄ intoxication (**Fig.2E**). Since, hepatotoxicity mediated by CCl₄ causes centrilobular cell death in hepatocytes and TGF β *per se* has a proapoptotic role on hepatocytes; we determined the occurrence of apoptosis. Two methods were used; terminal deoxynucleotidyl transferase dUTP nick end labeling (TUNEL) and activation of cleaved caspase 3, which occurs in apoptotic cells either by exogenous (death ligand) or endogenous (mitochondrial) pathways²⁹. TUNEL positivity indicates cell death; however, it cannot distinguish necrosis from apoptosis events. TUNEL activity was observed earlier (24 hrs after CCl₄) (**Fig.3**) than cleaved caspase 3 positivity (peak at 48 hours after CCl₄, **Fig.S4**). TUNEL positive cells were quantified in all the mice of each group throughout the time course (day 1- day 3) of regeneration (**Fig.3B**). Only at the earliest time point (1 day after CCl₄/ CCl₄+LY), there is significant TUNEL activity (**Fig.3A**), compared to the positive control. CCl₄+LY group has decreased number of dead cells compared to CCl₄ group at day 1 (**Fig.3B**). Activation of pro apoptotic protein caspase 3 in hepatocytes as detected by immunofluorescence has slightly different pattern (**Fig.S4A-B**) than TUNEL activity. It remains uncertain whether cleaved caspase 3 is expressed only by hepatocytes or HSCs in the damaged central vein area as indicated by α SMA+ HSCs (**Fig. S4B**). Quantification of cleaved caspase 3 positive areas during day 1– day 3 after damage induction shows a similar or slightly increased trend (non-significant at day 1, day 2) of caspase 3 activity in the LY-treated group, compared to CCl₄ (**Fig.S4C**).

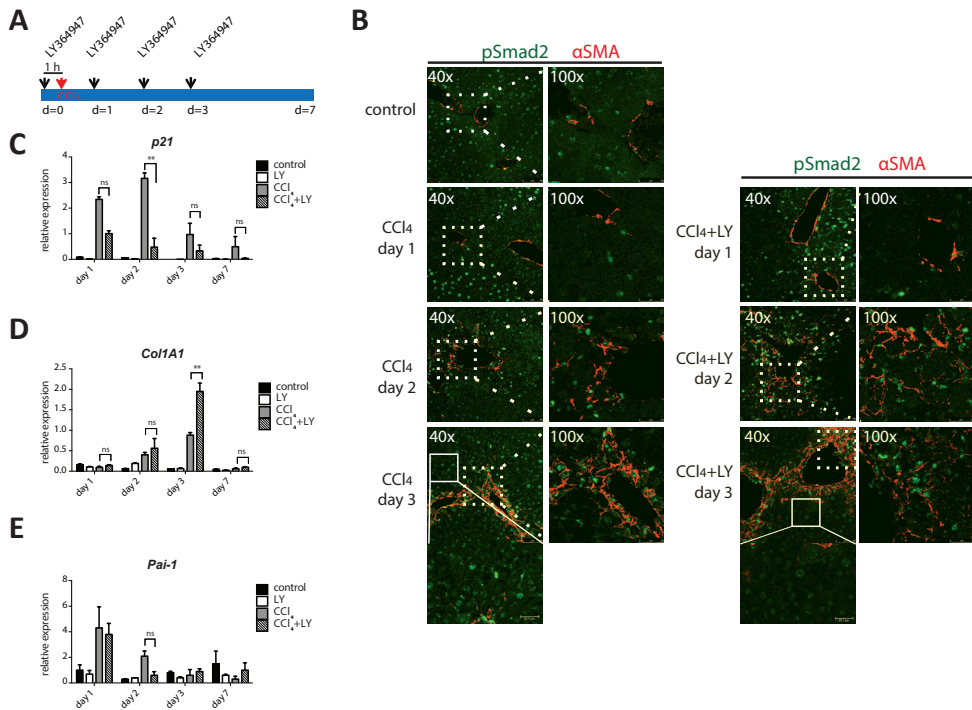


Fig.2. Dynamics of hepatic pSmad2 expression in the central vein area after LY364947 administration

(A). Scheme of experimental plan. Induction of acute liver damage by single shot of hepatotoxic agent CCl_4 took place at day 0. ALK5 inhibitor LY364947 (LY) was administered every 24 hours (d0-d3). d; day. (B). Time course of pSmad2 (green) and αSMA (red) expression by immunofluorescence during acute liver damage. Representative images of liver tissues from vehicle control, CCl_4 , and CCl_4 +LY injected mice. Images are shown at magnification 40x (scale bars= 50 μm). The marked area (dashed line) is shown at higher magnification (100x), scale bars= 25 μm . The non-dashed marked area is shown at higher magnification, scale bars= 22.7 μm . Time course (1, 2, 3, 7 days). (C). QPCR analysis of mRNA levels of *p21*, (D). *Col1A1*, (E). *Pai-1*; direct target genes of TGF β pathway. Treatment groups: Control (n=2), LY (n=2), CCl_4 (n=2), CCl_4 +LY (n=3). Error bars indicate S.E.M. Relative expression values were normalized to *Gapdh* expression. Time point: 48 hours after CCl_4 . LY; LY364947. **Statistically significant, $p < 0.01$. ns; non-significant difference.

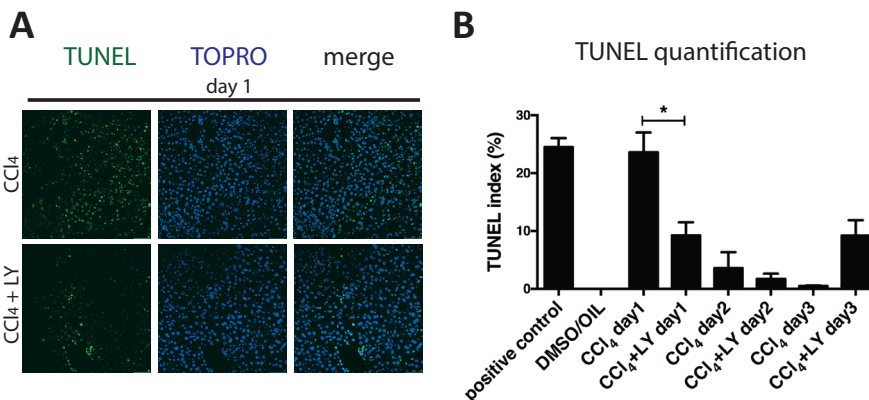


Fig.3. Effects of LY364947 on apoptosis in CCl₄-induced regeneration in mice

(A). The presence of TUNEL positive cells was determined by immunofluorescence at 24 hours after CCl₄ +/- LY. Representative images are shown per condition. Nuclei were visualized with TOPRO-3 (blue). Scale bars= 50 μ m. (B). Quantification of TUNEL immunofluorescence during day 1– day 3. Values are expressed as mean percentage of positive cells measured in multiple areas of liver sections from 2 mice/ CCl₄ group and 3 mice/ CCl₄+ LY group. Error bars represent \pm SEM. DNase I-treated sections were used as positive control for DNA fragmentation and TUNEL activity. *Statistically significant, $p < 0.05$. LY; LY364947

Effect of CCl₄ and LY administration on expression of pericentral hepatocyte markers

Cytochrome 450 enzyme CYP2E1 and Glutamine synthetase (GS) are expressed exclusively in a subpopulation of hepatocytes of the mouse liver, specifically located around the central veins (pericentral hepatocytes). CYP2E1-expressing hepatocytes are affected by CCl₄ because CYP2E1 converts it into a highly reactive radical (CCl₃OO) which causes severe oxidative stress and might lead to apoptosis. Upon CCl₄, *Cyp2e1* (Fig.4A) and *Gs* mRNA levels (Fig.4B) are decreased, indicating either cell death of this subset of hepatocytes or temporary switching off of gene transcription. In fact, inhibition of Cyp450 enzyme activity may limit cell death and tissue damage. At seven days after CCl₄ intoxication, mRNA levels of *Cyp2e1* (Fig.4A) and *Gs* begin to recover (Fig.4B); however, they do not reach the levels of the control groups (Fig.4A-B). Recovery of the damaged hepatocytes seems improved in the LY treated group; mRNA expression levels of *Cyp2e1* (Fig.4A) and *Gs* (Fig.4B) resemble the normal levels by day 7, in contrast to CCl₄ d7 group. In view of these data, we assessed the CCl₄-induced toxicity and recovery of CYP2E1+ hepatocytes by immunofluorescence in the damaged area *in situ*. Dynamics in protein expression of CYP2E1 (Fig.4C) follow similar pattern as the mRNA expression after CCl₄ (Fig.4A), indeed confirming that normalisation of zonation in the CV area by day 7 (Fig.4C) is improved after LY inhibitor. Despite cell death events induced by CCl₄ (Fig.3; Fig.S4), it is noteworthy that Cyp2E1 positive cells remain in the damaged area throughout the acute phase of injury (Fig.4C). Cells expressing α SMA, such as HSCs and smooth muscle cells, seem to intermingle with Cyp2E1+ hepatocytes (Fig.4C).

Inhibition of TGF β *in vivo* enhances hepatocyte regeneration

Cell proliferation is a mechanism for replenishment of hepatocytes as well as expansion of repair cells such as HSCs. We determined the expression of distinct proliferation markers (PH3 and PCNA) in CCl₄-induced liver damage (Fig.5). Histone 3 becomes phosphorylated only upon entry of the cell into mitosis; therefore phospho-histone 3 (PH3) expression is a marker of cell division (Fig.5A). Proliferating nuclear antigen (PCNA) is induced during duplication of DNA (S phase) prior to mitosis and also during DNA repair. Proliferation of hepatocytes is rare in the normal liver as they are quiescent cells (Fig.5S), however, upon injury they can re-enter cell cycle (Fig.5A-C). Quantification of PH3 indicates higher proliferation in presence of the LY inhibitor (Fig.5B). PH3 positive cells are mainly α SMA positive HSCs upon CCl₄ (Fig.5A), however, proliferating α SMA-negative cells were also observed in the CCl₄+LY liver tissues (Fig.5A), which are likely dividing parenchymal cells. Overview images of the same liver area were acquired with lower magnification for comparison (Fig.5S). S phase marker PCNA is increased in the CCl₄+LY group compared to the CCl₄ group in HSCs and hepatocytes around the central vein area, adjacent to necrotic cells which express cleaved caspase 3 protein (Fig.5C). Proliferating cells that are distant from the central veins are

morphologically hepatocytes (Fig.5C). Quantification of overall number of PCNA positive cells as measured by immunofluorescence in the whole liver tissue showed increased trend of proliferation in the CCl₄+LY group, particularly at day 2 and day 3 (Fig.5D). Western blotting analysis in whole liver extracts also confirmed that LY-treated samples had higher PCNA expression (Fig.5E). Administration of LY seems to inhibit the total levels (whole liver) of cyclin-dependent kinase inhibitor p21 (Fig.5E) which halts cell cycle progression in G1 phase and is regulated directly by TGFβ^{13,14}.

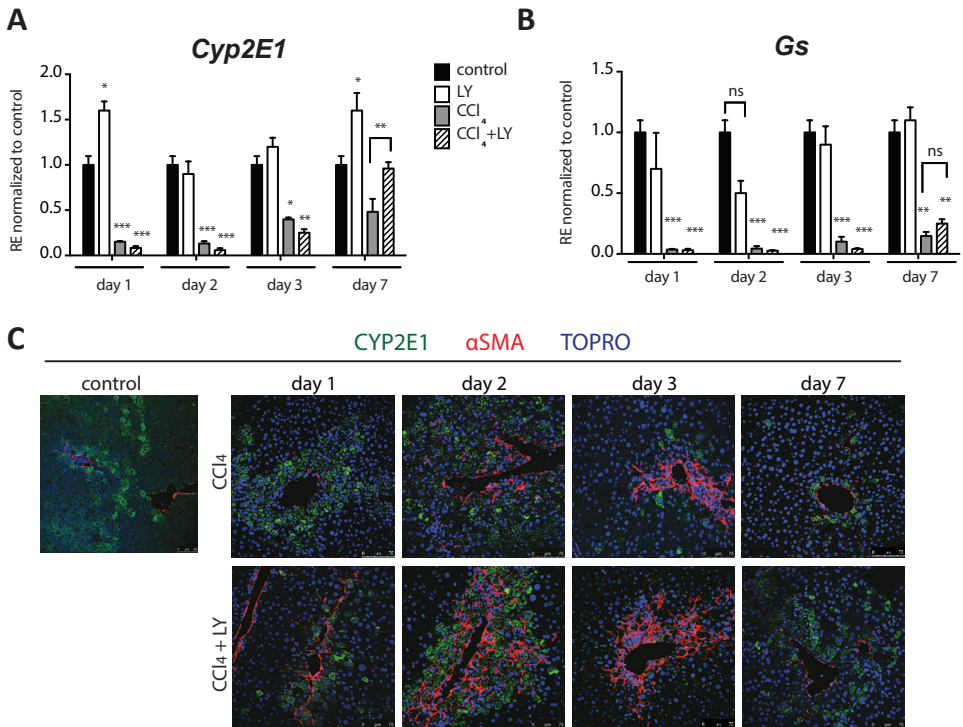


Fig.4. Hepatic CYP2E1 expression of central hepatocytes is sustained in the damaged area during acute liver injury

Analysis of central hepatocyte-specific transcripts by QPCR in whole liver cDNA preparations. (A). *cytochrome 450 2E1 (CYP2E1*, pericentral hepatocytes), (B). *glutamine synthetase (Gs*, pericentral hepatocytes). Treatment groups: Control (n=2), LY (n=2), CCl₄ (n=2), CCl₄+LY (n=3). Error bars indicate S.E.M. Expression values were normalized to *Gapdh* expression and to the control sample (vehicle DMSO/oil). Time point; d1: day 1 after treatment, d2: day 2 after treatment, d3: day 3 after treatment, d7: day 7 after treatment. *Statistically significant, p<0.05, **Statistically significant, p<0.01, *** Statistically significant, p<0.001 versus control, ns; non-significant difference. (C). Immunofluorescence staining of central hepatocytes (CYP2E1, green), activated HSCs and vascular smooth muscle cells (αSMA, red) in the central vein area. Nuclei are visualized with TOPRO-3 (blue). Time points: day 1, day 2, day 3 and day 7 after CCl₄ or CCl₄+LY. LY; LY364947. Magnification: 40x. Scale bars= 75μm.

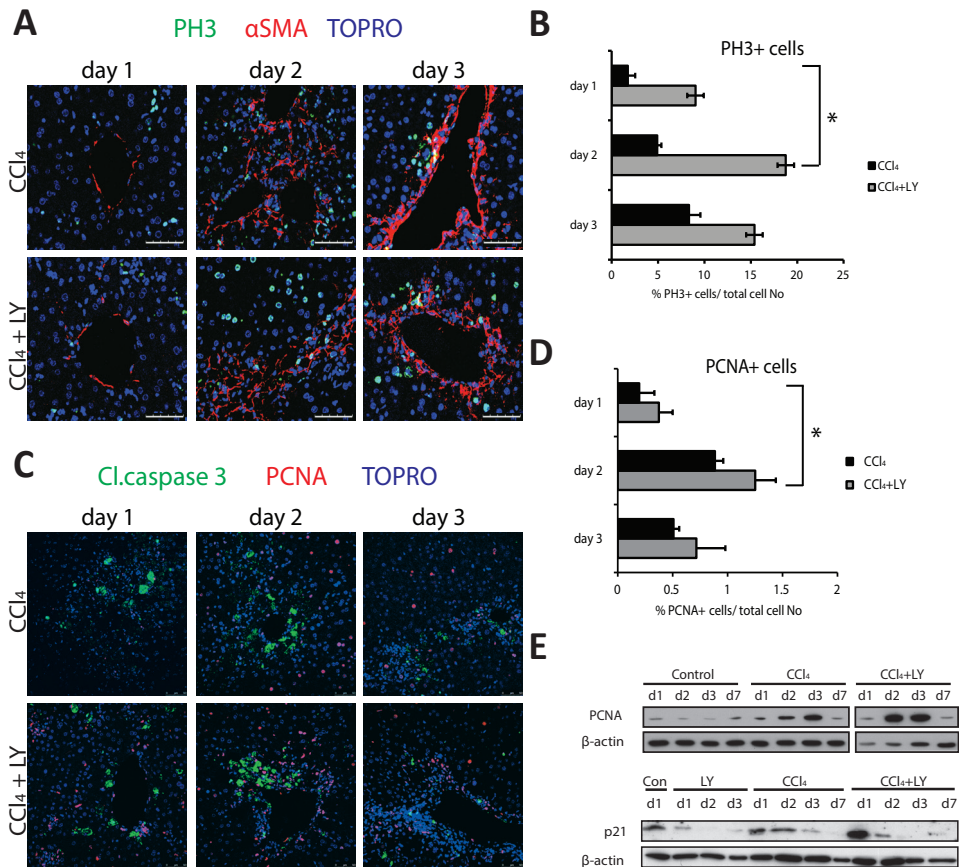


Fig.5. Increased cell proliferation after LY364947 administration in CCl₄-induced regeneration in mice (A). Mitotic events after CCl₄ and in combination with LY, as determined by immunofluorescence for phosphorylated histone protein 3 (PH3, green) in the damaged central vein area (αSMA, red). A representative image is shown per condition. Nuclei are visualized with TOPRO-3 (blue). Scale bars: 100μm. (B). Quantification of PH3 positive cells during day 1- day 3, expressed as mean percentage of positive cells from 2 animals/ CCl₄ group and 3 mice/ CCl₄+LY group. Error bars represent ± SEM. (C). Co-labeling of apoptotic and proliferating cells in the damaged central vein area; activation of proapoptotic protein caspase 3 in hepatocytes, as detected by immunofluorescence (cl.caspase 3, green) and DNA synthesis marker PCNA (red) after CCl₄+/-LY administration. Scale bars: 50μm. (D). Quantification of PCNA positive cells as mentioned previously. (E). Protein expression of PCNA and p21 as measured by immunoblotting in whole liver tissue extracts. Treatment groups: Control (DMSO-oil), CCl₄, CCl₄+LY. Time course: day 1 (d1), day 2 (d2), day 3 (d3), day 7 (d7) after CCl₄ injection and small molecule inhibitor administration (day 0- day 3). β- actin was used as protein loading control. LY; LY364947. *Statistical significance, p<0.05.

In vivo interference of TGFβ pathway by LY does not inhibit activation of HSCs in the acute liver damage model

To assess beneficial or adverse effects of LY on wound healing response, we have performed extensive histological analyses. Induction of αSMA is a reliable marker of liver MFBs (activated HSCs), as well as MFBs resident in other tissues and vascular smooth muscle cells. To distinguish HSC-enriched genes we measured the expression of αSMA and *Ctgf* which are enriched in HSCs. αSMA (Fig.S7A) and *Ctgf* (Fig.S7B) mRNA levels show a decreasing

trend of expression in the CCl₄+LY compared to the CCl₄ group. In the control groups, α SMA expression was only present in the smooth muscle cells lining portal and central veins (**Fig.S1**). Mice administered with CCl₄ toxin show signs of wound healing response during the first 48 and 72 hours (day 2, 3), with up regulation of α SMA protein, as observed by immunofluorescence (**Fig.S8A**) and by western blot analysis (**Fig.S8C**). Tissue restoration after CCl₄-induced damage takes place by day 7, when α SMA protein expression is decreased back to basal levels (**Fig.S8A**). However, expression of α SMA protein as measured by western immunoblotting in whole liver protein samples (**Fig.S8C**) is similar or slightly higher in livers of the CCl₄+LY group over the CCl₄ group. Quantification of positive staining in individual mice per group reflects a trend for higher induction of α SMA protein in the CCl₄+LY group (**Fig.S8B**); therefore, HSC activation might not be affected by the LY treatment.

In vitro effects of LY on TGF β signaling

The differential *in vivo* responses of HSCs and hepatocytes to the LY were furthermore examined using established *in vitro* mouse cell lines. Mouse HSCs and AML12 (hepatocytes) cells were stimulated with TGF β or with TGF β +LY and the expression of TGF β downstream targets was tested by QPCR and western blotting. As control, non-treated cells and TGF β -stimulated cells were used. TGF β stimulation of HSCs up regulates mRNA expression of α SMA compared to non-stimulated HSCs (**Fig.S9**). TGF β inhibition in HSCs is time- and dose-dependent; at high doses LY (5 μ M LY, 10 μ M LY) abrogates the effect of TGF β stimulation on α SMA (**Fig.S9**). However, at lower dose (1 μ M) LY seems to induce, rather than inhibit, the TGF β -mediated effect on α SMA expression, particularly at later (20 hrs TGF β +1 μ M LY) time points (**Fig.S9**). We measured the expression of direct target genes *Pai-1* and *Ctgf* on HSCs and hepatocytes; cell type- specific differences are observed during early induction by TGF β (after 1 hour) (**Fig.S10**). LY treatment might be more efficient in inhibiting *Pai-1* expression in AML12 hepatocytes (**Fig.S10C**) rather than in HSCs (**Fig.S10A**). Similarly, *Ctgf* expression is efficiently down regulated in the AML12 cells as early as 1 hour (**Fig.S10D**) while *Ctgf* levels in HSCs remain high at 1 hour in presence of LY inhibitor (**Fig.S10B**). Furthermore, phosphorylation of Smad2 (**Fig.S11A-B**) and Smad3 (**Fig.S11D-E**) was analysed in a dose- dependent way after TGF β stimulation (1 hour) and inhibition with LY (1 μ M, 5 μ M, 10 μ M). HSCs (**Fig.S11A, D**) and AML12 cells (**Fig.S11B, E**) *in vitro* respond to addition of exogenous TGF β by induction of downstream pSmad2 and pSmad3. Quantification of protein bands using densitometry was done in three independent experiments, and showed that decrease of phosphorylated Smad2 (**Fig.S11C**) and Smad3 (**Fig.S11F**) levels is analogous to the concentration of LY, with 10 μ M dose being the most effective for both HSCs and AML12 cell types.

Discussion

Acute liver failure is a severe condition of extensive hepatocyte necrosis and improper wound healing response, which occurs by exposure to intoxicants such as acetaminophen, thioacetamide, chloroform and CCl₄. TGFβ is an inhibitory factor of liver regeneration by causing cytostatic response on hepatocytes and profibrotic effects on HSCs. Taking into account the deregulated levels of TGFβ in many fibrotic and malignant diseases we have investigated the impact of short term inhibition of TGFβ pathway on CCl₄-induced acute damage and liver regeneration *in vivo*.

In this study we assessed the distinct roles of TGFβ in cell death and regeneration of different cell types upon acute liver damage in mice. CCl₄-induced toxification occurs mainly in the central vein area, probably due to the low oxygen pressure and high cytochrome 450 enzyme levels³. Chemicals that induce cytochromes that metabolize CCl₄ or delay tissue regeneration when co-administered with CCl₄ will potentiate its toxicity, while appropriate CYP450 inhibitors will limit its toxicity⁶. Upon CCl₄, TGFβ canonical pathway is activated and target genes *p21*, *Col1A1*, *Pai-1*, *αSMA* and *Ctgf* are induced. However, histology of the liver tissues showed a local inhibition of pSmad2 early upon tissue injury, exclusively in the centrilobular hepatocytes but not in the activated HSCs. This particular cell response may play a role in reentering of quiescent hepatocytes into the cell cycle and perhaps, initiation of the regenerative response. This observation is in line with previous studies^{12,14} describing transient desensitization of hepatocytes to TGFβ-mediated growth arrest. Inhibition of ALK5 kinase activity by LY appears to have a potential stimulatory effect on hepatocyte proliferation during liver regeneration. Hepatocyte proliferation rate, indicative of the replacement of damaged cells by newly formed cells, was measured by PCNA immunostaining and western blotting. Proliferation is stimulated by LY co-administration with CCl₄ as suggested by the increased PCNA levels as well as higher levels of the mitosis marker phosphorylated histone³. Mitotic events are very few after CCl₄ intoxication, although this S phase marker expression is induced. A possible explanation for this difference is that hepatocytes are frequently binuclear cells since they progress through the DNA duplication phase but do not undergo cell division³⁰. Higher proliferation rate after LY treatment is observed as early as 24 hours after injury, which may suggest that this compound leads to faster activation of innate repair and regeneration responses. Similar to our data, suppression of TGFβ induces transcription of regeneration factors (HGF, IL-6) in dimethylnitrosamine-induced chronic liver injury in rats¹⁸. Enhanced proliferation of hepatocytes, observed in the presence of dominant negative TGFβ receptor mutants¹⁸ and hepatocyte specific conditional deletion of TGFβRII³¹ supports the hypothesis that TGFβ sustains quiescent hepatocytes in a differentiated state. Cell death of a subset of hepatocytes occurs immediately due to CCl₄ toxicity; however, there is clearly a subpopulation of Cyp2E1 hepatocytes that remain in the central vein zone at 24 hours after CCl₄. The location of these cells adjacent to the central vein may suggest that the damaged cells have the capacity to survive and to sustain their initial location and hepatocyte specific gene expression. This observation is in line with *Cyp2E1* mRNA presence in centrilobular hepatocytes as shown by *in situ* hybridisation in regenerating mouse liver³². *Cyp2E1* zonal expression is normalized to the basal levels by day 7 in the LY-treated group, indicative of better recovery of the damaged area. LY may also possibly limit the damage or necrosis as suggested by the lower levels of TUNEL activity at 24 hours after CCl₄ intoxication. However, cleaved caspase 3 levels are similar in CCl₄ and CCl₄+LY and peak at a later time point than TUNEL activity; the different pattern of terminal deoxynucleotidyl transferase

(TdT) and Caspase 3 expression suggests the presence of two different cell populations and functional processes. TUNEL positive cells, which are evident at early time points, possibly represent the cells undergoing necrosis due to the toxin, while activated Caspase 3 marks cells undergoing apoptosis.

One consideration regarding HSCs is their activated MFB characteristics, such as α SMA and COL1A1 expression, which are sustained by autocrine TGF β signaling, however, due to the terminally differentiated phenotype, HSCs might not act in response to exogenously provided TGF β stimulation³³. Furthermore, other studies have shown that ALK4, ALK5 and ALK7 receptors can be targeted by SB-431542 kinase inhibitor, which blocks TGF β -induced nuclear translocations of Smad3 and Col1A1 levels in renal epithelial carcinoma, HaCat, NIH 3T3 and C2C12 cells^{28,34,35}. Molecular ALK5 inhibition has been shown by the use of LY364947 compound^{30,36,37} or by other inhibitors, e.g. GW6604³⁸, GW788388³⁹. Selectivity of the inhibitors is dose-dependent and inhibition of TGF β receptor kinase activity may not inhibit non-Smad signaling response which may lead to adverse effects⁴⁰.

The *in vivo* co-administration of LY364947 in CCl₄-mediated liver injury potently seems to decrease the mRNA expression of direct target genes, however since whole liver (hepatic) extracts have been used in this study, the cell type-specific enrichment of target genes cannot be determined. Ctgf, p21 are expressed by parenchymal and non-parenchymal cell types⁴¹⁻⁴³. Genes that are typically expressed in HSCs, such as Col1A1 and α SMA, have similar mRNA and protein levels in CCl₄ and CCl₄+LY-injected mice. Expression of *Pai-1* is not significantly different in CCl₄+LY-injected mice compared to CCl₄. In the model of acute hepatic injury used in this study, either HSC cell population is not sensitive to ALK5 receptor inhibition³³ after injury response is initiated or TGF β inhibition is compensated by other signaling pathways (e.g. PDGF 1, p38 MAPK³⁴). In fact, α SMA is directly regulated by TGF β and canonical Smad signaling^{12,15,16}. Id1 target gene of BMP signaling, which is also induced by TGF β 1/ ALK1/Smad1 branch, is important for activation of HSCs and actin polymerization⁴⁴. Thus, TGF β inhibition alone might not be sufficient to abrogate HSC proliferation and/ or accumulation of these cells. Enhanced fibrogenesis is beneficial for the regenerative response; however, if it becomes uncontrollable it may eventually lead to fibrosis. Thus, HSCs may require cell-specific targeting or longer treatment with ALK5 inhibitor in order to invert their fibrogenic properties in fibrosis studies^{36,45}. The study of van Beuge *et al.*, 2013 showed that administration of LY without cell-specific delivery is less effective in decreasing the levels of fibronectin or collagen, similarly to our data. Other *in vivo* studies have provided evidence on the efficiency of the LY inhibitor in interstitial heart fibrosis⁴⁶ and in lymphangiogenesis in a chronic peritonitis mouse model⁴⁷. In cancer studies, combined administration of LY and Imatinib prolongs the survival of mice with chronic myeloid leukemia⁴⁸. Nevertheless, specific targeting of a TGF β inhibitor in any disease setting is definitely advantageous over systemic administration in order to prevent on target responses that might be disadvantageous due to the differential role of TGF β depending on the cell type/ gene expression context. An interesting hypothesis that might emerge from the analysis of our data that requires further investigation is that the damaged hepatocytes survive and remain functional under acute toxin injury condition. Thus, cell damage might not *de facto* lead to cell death and massive hepatocyte necrosis and should be carefully characterised in the different experimental models of hepatic injury. *In vivo* TGF β inhibition by systemic administration of the LY appears to enhance hepatocyte proliferation and regeneration of the liver, thus it could be therapeutically beneficial to explore cell type-specific targeting depending on the liver disease context e.g. hepatocyte

or HSC-specific delivery for hepatocellular carcinoma or fibrosis, respectively.

Acknowledgements

This study was supported by Netherlands Organization for Scientific Research (NWO-MW), Netherlands Institute for Regenerative Medicine (NIRM). This work was also supported in part by Marie Curie Initial Training Network (ITN) IT-Liver grant. We thank our colleagues, Dr. Boudewijn Kruithof and Prof. B. van de Water for valuable advice and discussion and Dr. David Scholten for the Col-GFP HSC cell line.

Conflict of interest

The authors declare no conflict of interest

Supplementary figures

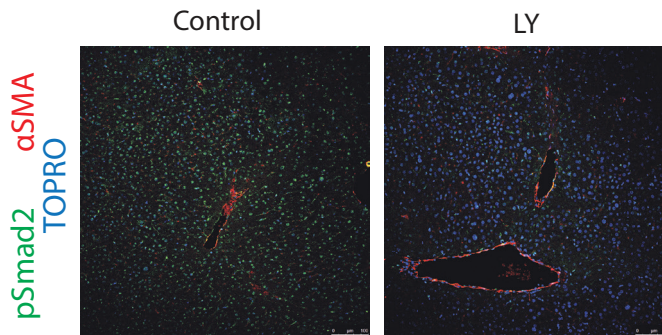


Fig.S1. LY364947 efficiently blocks Smad2 phosphorylation in normal liver

Staining for phosphorylated Smad2 (pSmad2, green) and alpha smooth muscle actin (αSMA, red) in control (DMSO-oil) and LY groups. LY; LY364947. 24 hours post injections. Nuclei were visualised by TOPRO-3 (blue). Magnification 20x. Scale bars= 100 μm.

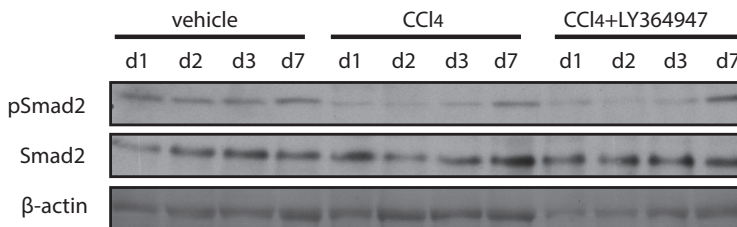


Fig.S2. Phosphorylated and total Smad2 protein levels in whole liver homogenates

Protein expression of pSmad2 and total Smad2 was measured by western immunoblotting in whole liver tissue extracts. Total Smad2 was detected using an antibody that recognizes the total Smad2 and Smad3 proteins. Treatment groups: vehicle (DMSO-oil), CCl₄, CCl₄+LY364947. Time course: day 1 (d1), day 2 (d2), day 3 (d3), day 7 (d7) after CCl₄ injection and small molecule inhibitor administration (day 0- day 3). β- actin was used as protein loading control.

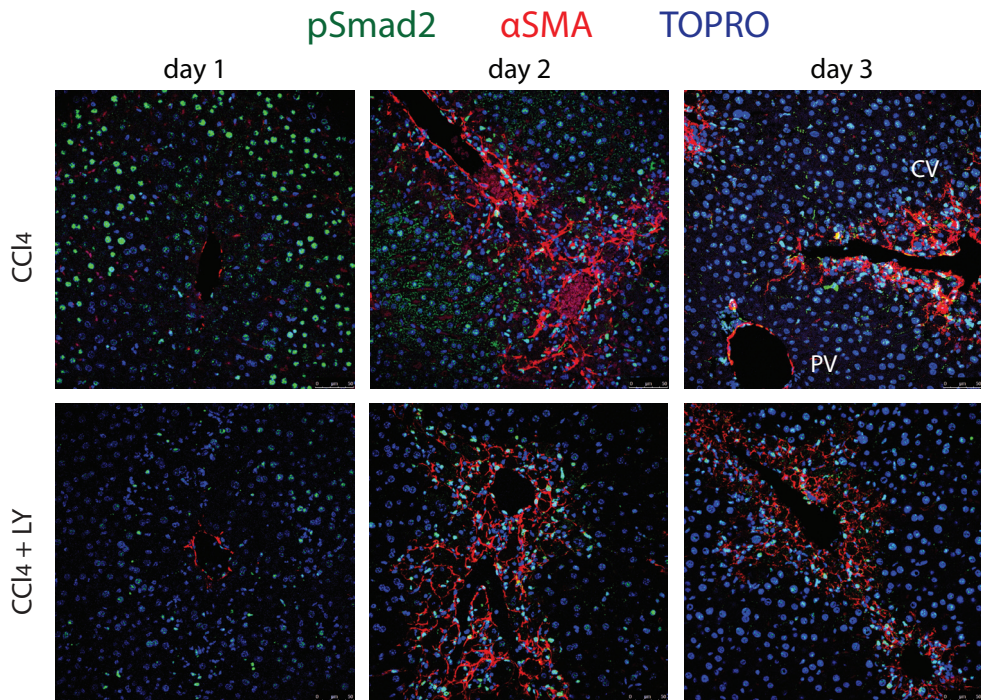


Fig.S3. LY364947 efficiently blocks Smad2 phosphorylation in hepatocytes but not in αSMA- positive HSCs
 Time course (day1, day2, day3) of Smad2 phosphorylation by immunofluorescence staining (green) in liver tissues from animals that received CCl₄, CCl₄+LY. αSMA staining (red) marks activated HSCs (liver MFBs) as well as vascular smooth muscle cells. Nuclei were visualized by TOPRO-3 (blue). Representative images are shown per treatment group and time point. Magnification 40x, Scale bars= 50 μm. LY; LY364947.

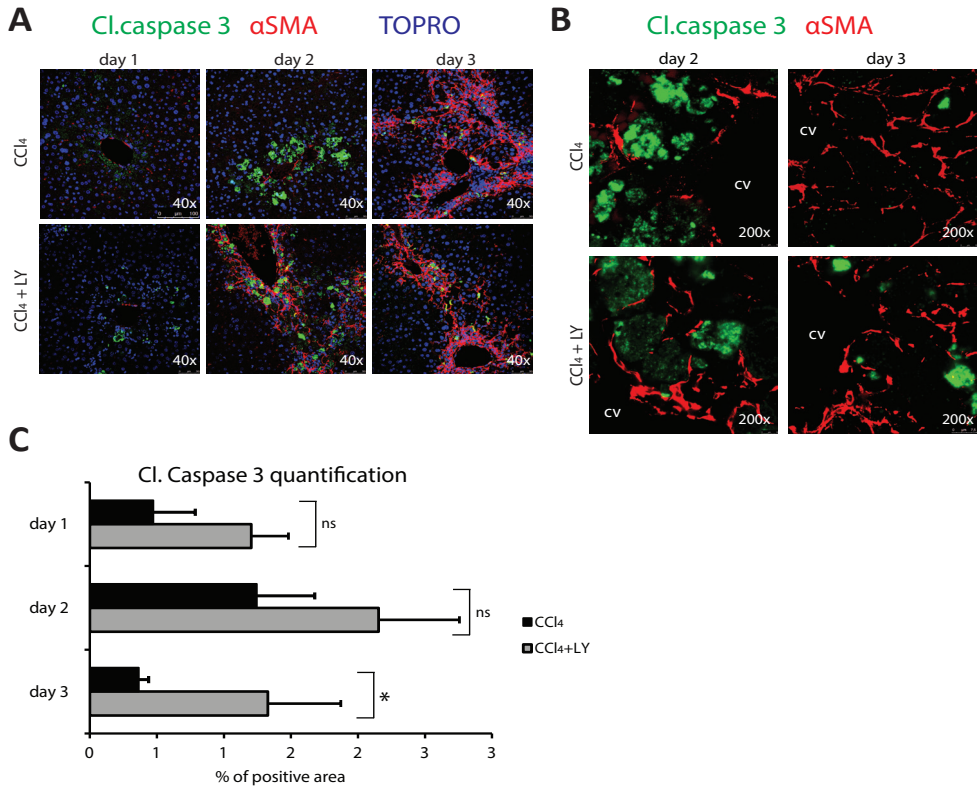


Fig.S4. Apoptosis marker cleaved caspase 3 expression

(A). Activation of proapoptotic protein caspase 3 in hepatocytes as detected by immunofluorescence (cleaved (Cl) Caspase 3, green) after CCl₄+/- LY364947 administration in the damaged central vein area as indicated by αSMA+ HSCs (red). Nuclei were visualised by TOPRO-3 (blue). Magnification 40x. Scale bars= 50µm. (B). Cleaved caspase 3 (red) and αSMA (red) immunofluorescence of sections at higher magnification (200x) on day 2 and day 3 after CCl₄-induced injury. cv; central vein Scale bars= 5 µm. (C). Quantification of cleaved caspase 3 positive area during day 1– day 3 after damage induction. Different fields of view in stained sections for every individual mouse were imaged and quantified. Graph indicates the mean percentage of positive stained area from 2 mice/ CCl₄ group and 3 mice/ CCl₄+LY group. Error bars represent ± SEM. *Statistical difference (P<0.05). ns; non-significant difference. LY; LY364947.

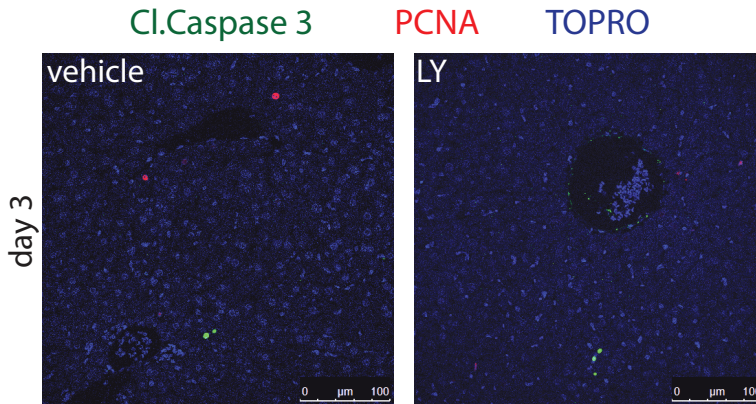


Fig.S5. PCNA and cleaved caspase 3 levels in quiescent control liver tissues

Time point; after 3 days of vehicle (left) or LY (right) administration. LY; LY364947. Cleaved (Cl) caspase 3; marker of apoptosis (green), PCNA; marker of proliferation (red). Nuclei were visualized with TOPRO-3 (blue). Scale bars= 100μm.

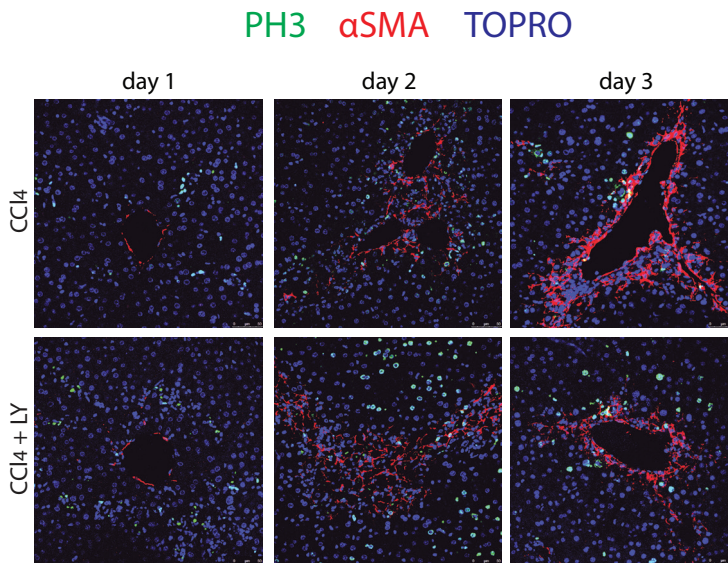


Fig.S6. PH3 immunofluorescence

Mitotic events after CCl₄ or in combination with LY364947 (LY), as determined by immunofluorescence for phosphorylated histone protein 3 (PH3, green) in the damaged central vein area (αSMA+ HSCs and smooth muscle cells, red). A representative overview image is shown per condition. Nuclei were visualized with TOPRO-3 (blue). Magnification 40x. Scale bars = 50μm.

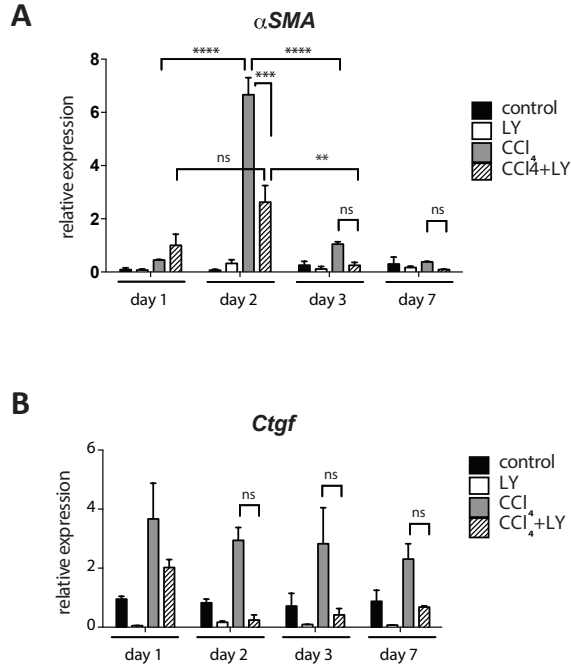


Fig.S7. Hepatic α SMA and Ctgf mRNA levels after CCl₄ administration in presence or absence of LY364947 inhibitor

(A). mRNA levels of α SMA and (B). mRNA levels of Ctgf as measured by QPCR. Treatment groups: Control (n=2), LY (n=2), CCl₄ (n=2), CCl₄+LY (n=3). LY; LY364947. Error bars indicate S.E.M. Relative expression values were normalized to *Gapdh* expression. Time points: day 1- day 2- day 3- day 7 after CCl₄. **Statistically significant, p<0.01, ****Statistically significant, p<0.0001, ns; non-significant difference.

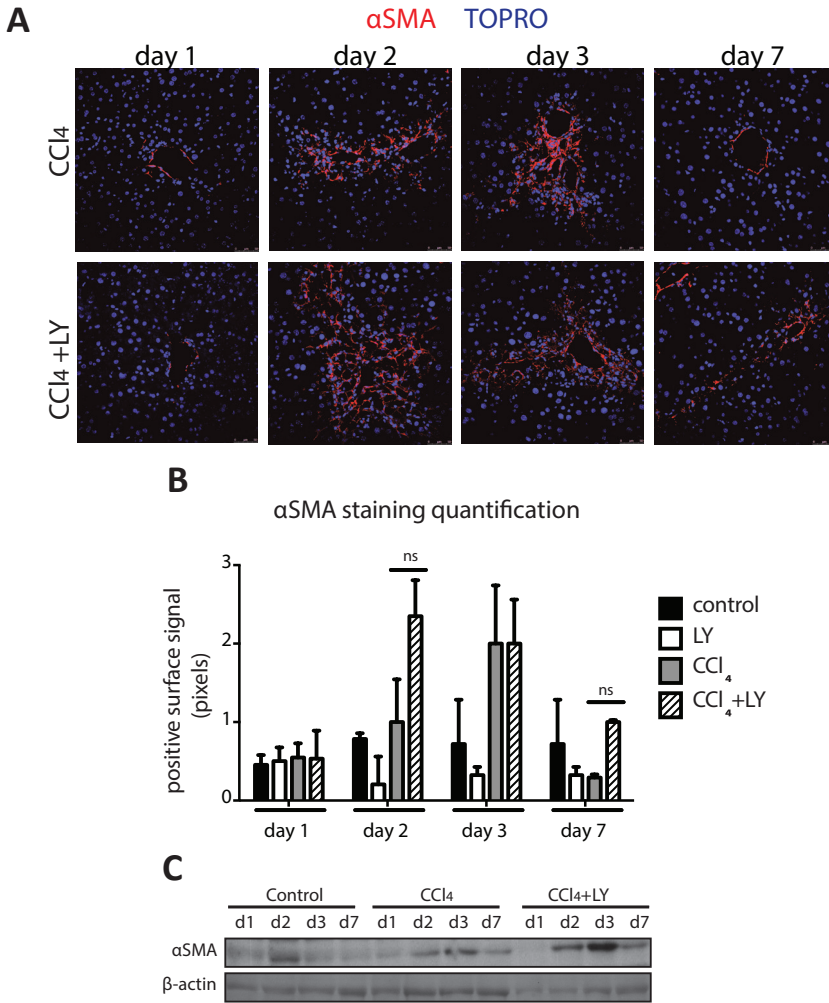


Fig.S8. In vivo inhibition of TGFβ receptor kinase activity in acute liver damage model by small molecule inhibitor LY364947

(A). Immunofluorescence staining of αSMA+ HSCs in CCl₄ and CCl₄+LY treated liver tissues. Representative images are shown per each time point; day 1, day 2, day 3 and day 7 after single CCl₄ dose. Nuclei were visualized by TOPRO-3 (blue). Magnification 40x. Scale bars= 50 μm. (B). Quantification of αSMA immunofluorescence in liver tissues. Error bars represent S.E.M. Time points: day 1, day 2, day 3, day 7 after CCl₄ shot. Treatment groups: control (n=2 per time point), LY (n=2), CCl₄ (n=2) and CCl₄+LY (n=3). ns; non-significant difference. (C). Protein expression of αSMA measured by western immunoblotting from whole liver tissue extracts. β- actin was used as protein loading control. Time points and treatment groups as described previously. LY; LY364947.

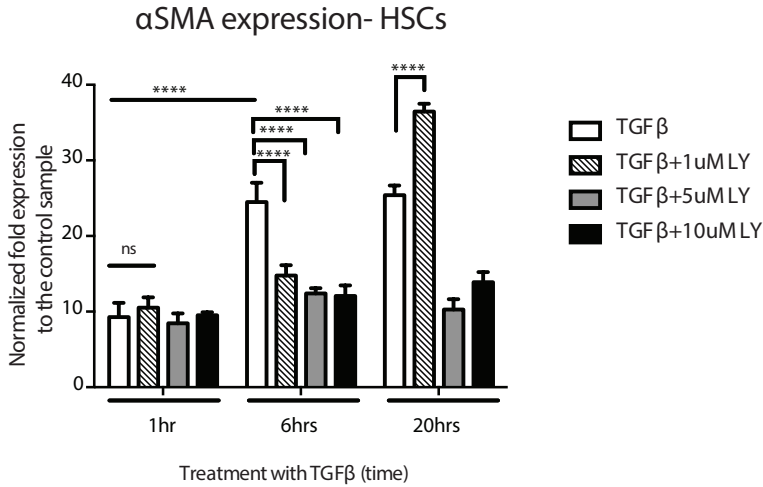


Fig.S9. High dose of LY364947 treatment is required to inhibit αSMA expression in HSCs *in vitro*
 Quantitative PCR analysis of αSMA expression in HSCs. Cells were pretreated with increasing concentrations of LY364947 (LY 1uM, 5uM, 10uM) for 1 hour and stimulated with TGFβ3 (5ng/ml) for 1, 6 and 20 hours. Expression was normalized to the values of the control cDNA from non-stimulated cells. ****Statistically significant, p<0.0001 versus TGFβ. ns; non-significant difference.

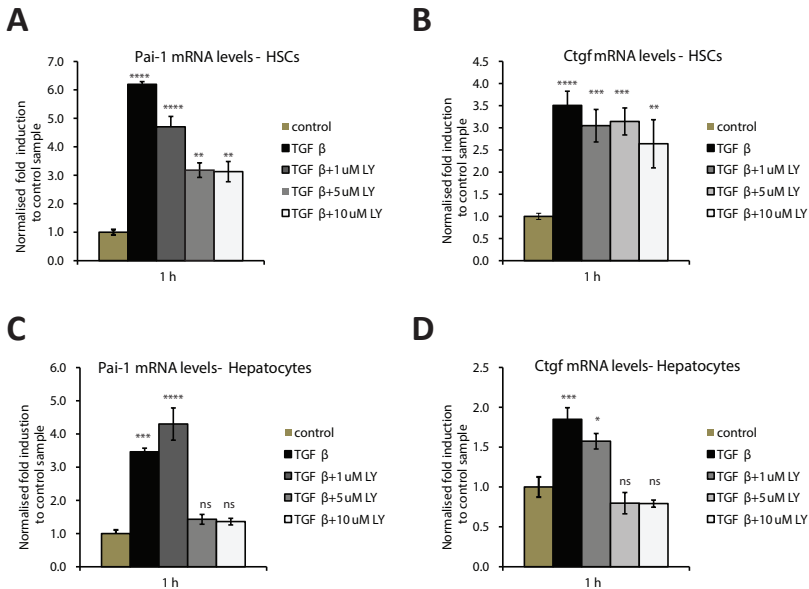


Fig.S10. *In vitro* effects of LY364947 on TGFβ target genes in HSCs and hepatocyte AML12 cell line
 (A). *Pai-1* mRNA expression and (B). *Ctgf* mRNA expression in mouse HSCs. HSCs were pretreated with increasing concentrations of LY364947 (LY 1uM, 5uM, 10uM) and stimulated with TGFβ3 (5ng/ml) for 1 hour. Fold induction ($\Delta\Delta Ct$) was normalized to the control sample (non-stimulated cells) and *Gapdh* expression values. (C). *Pai-1* mRNA and (D). *Ctgf* mRNA expression in mouse AML12 hepatocytes. Cells were pretreated with increasing concentrations of LY364947 (LY 1uM, 5uM, 10uM) and stimulated with TGFβ3 (5ng/ml) for 1 hour. Fold induction ($\Delta\Delta Ct$) was normalized to the control sample (non-stimulated cells) and *Gapdh* expression values. *Statistically significant, p<0.05, **Statistically significant, p<0.01, ***Statistically significant, p<0.001, ****Statistically significant, p<0.0001 versus control sample. ns; non-significant difference.

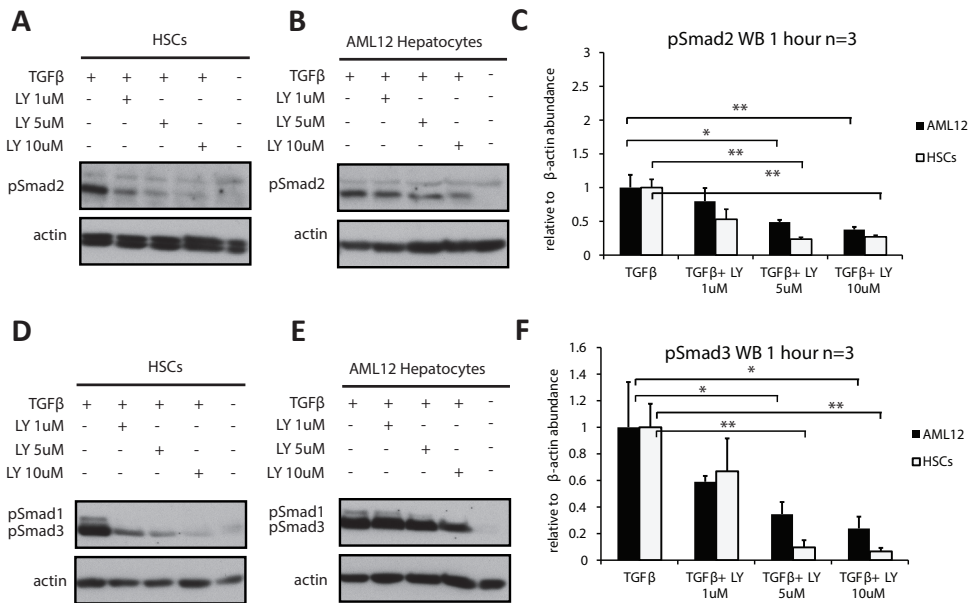


Fig.S11. In vitro effects of LY364947 on Smad2, Smad3 phosphorylation in HSCs and AML12 cell lines
 Cells were pretreated with increasing concentrations of LY364947 (LY 1 uM, 5uM, 10uM) for 1 hour and stimulated with TGFβ3 (5ng/ml) for 1 hour (n=3). Loading control; β-actin. (A). pSmad2 in HSCs (1h time point), (B). pSmad2 in AML12 hepatocytes (1h time point), (C). Quantification of western blotting pSmad2 signal by densitometry (n=3). Relative abundance over β-actin, (D). pSmad1, pSmad3 in mouse HSCs, (E). pSmad1, pSmad3 in mouse AML12 hepatocytes, (F). Quantification of western blotting pSmad1, 3 signal by densitometry (n=3). Relative abundance over β-actin. *Statistically significant, $p < 0.05$, **Statistically significant, $p < 0.01$ versus TGFβ.

Supplementary Materials and Methods

Immunofluorescence

Liver tissues were fixed in 4% paraformaldehyde solution overnight, washed in PBS and processed for paraffin embedding. For every mouse, one of the liver lobules was embedded in a paraffin block and multiple serial sections (0.6 μm) were prepared. For antigen retrieval, sections were boiled 10- 30 min in antigen unmasking solution (Vector Labs) and were incubated in 3% H₂O₂ for endogenous peroxidases sequestering. Sections were blocked with 1% bovine serum albumin (BSA)- PBS-0.1% v/v Tween 20) and incubated with primary antibodies diluted in the blocking solution, overnight at 4°C or room temperature. Primary antibodies and dilutions used are as follows: anti-αSMA 1:500 (Sigma), anti-phospho-Smad2 1:1000 (Cell Signaling), anti-Cyp2e1 1:500 (Biorbyt), anti-Fsp1 1:1000 (Millipore), anti-desmin 1:500 (Santa Cruz), anti-HNF4α 1:100 (Santa Cruz), anti-PCNA 1:10.000 (Sigma), anti-phospho Histone3 1:1000 (Millipore), anti-cleaved caspase 3 1:1000 (Cell Signaling). Sections were then incubated with secondary antibodies labeled with Alexa Fluor 488, 555, or 647 (Invitrogen/Molecular Probes, 1:250 in PBS-0.1% Tween 20). Detection of pSmad2 and Cyp2e1 was enhanced using tyramide amplification (Invitrogen/Molecular Probes) by incubation of slides with horseradish peroxidase (HRP)-conjugated secondary antibody (1:100 dilution) (Invitrogen/Molecular Probes), followed by incubation with tyramide-488 for 10 minutes. All sections were counterstained with TOPRO-3 (Invitrogen/Molecular Probes) at 1:1000 dilution in PBS-0.1% Tween20 for nuclei visualization, and mounted with Prolong G mounting medium (Invitrogen/Molecular Probes), which contains DAPI. Every immunofluorescence staining experiment was performed multiple times using different sections from the same lobule from every mouse.

RNA isolation, RT-PCR and Quantitative PCR

During liver tissue collection, one of the liver lobules of each individual mouse was snapfrozen in liquid nitrogen and stored at -80°C for RNA analyses. One liver part per mouse (100 μm) was homogenized using an UltraTurrax homogenizer (T25 basic, IKA) in TRIpure reagent (Roche) and directly processed for total RNA isolation according to the TRIpure RNA extraction protocol. Total RNA (0.5 μg) was used for first strand cDNA synthesis using RevertAid H Minus first strand cDNA synthesis kit (Fermentas). For quantitative PCR (Q-PCR) ten-fold diluted cDNA was amplified in a CFX Real Time Detection system (Bio-rad) using SYBR Green Supermix reagent (Bio-rad). Expression levels were normalized to housekeeping gene (Gapdh).

Primer sequences:

αSMA: *for*-ACTGGGACGACATGGAAAAG, *rev*- CATCTCCAGAGTCCAGCACA

Pai: *for*-GCCAACAAGAGCCAATCACA, *rev*-AGGCAAGCAAGGGCTGAAG

Cyp2e1: *for*- GGACATTCCTGTGTTCCAG, *rev*- CTTAGGGAAAACCTCCGCAC

Ctgf: *for*- CAGACTGGAGAAGCAGAGCC, *rev*- GCTTGGCGATTTAGGTGTC

Gs: *for*- CTCCTGACCTGTTACCCAT, *rev*- TTGCTTGATGCCTTTGTTC

Gapdh: *for*-AACTTTGGCATTGTGGAAGG, *rev*-ACACATTGGGGGTAGGAACA

p21: *for*- CGGTGTCAGAGTCTAGGGGA, *rev*- ATCACCAGGATTGGACATGG

Western immunoblotting

During liver tissue collection, one of the liver lobules of each individual mouse was snapfrozen in liquid nitrogen and stored at -80°C for protein analyses. One liver part per mouse (100 µm) was homogenized in tissue lysis buffer (30 mM Tris pH 7.4, 150 mM NaCl, 0.5% Triton-X 100, 10 mM NaF, 1 mM Na₃VO₄, 10mM EDTA pH=8.0, 1%SDS, plus complete protease inhibitors, Roche) using an Ultra Turrax homogenizer (T25 basic, IKA). Following a centrifugation step (15 min, 4000 rpm, 4°C) to remove debris, the protein extract can be collected (supernatant) and further diluted 5-fold with lysis buffer. Whole protein extract by DC protein assay (Biorad) using BSA serial dilutions in tissue lysis buffer. A total of 20 ug was diluted in 4x Laemml buffer, separated by SDS-PAGE and transferred to nitrocellulose membranes. The following primary antibodies were used anti-αSMA 1:1000 (Abcam), anti-phospho-Smad1 1:1.000 (Cell Signaling), anti-phospho-Smad2 1:1.000 (Cell Signaling), anti-Smad2/3 1:1000 (BD Biosciences), anti-PCNA 1:5000 (Sigma), anti-p21 (Santa Cruz), GAPDH 1:10.000 (Millipore), actin 1:10.000 (Sigma). Appropriate secondary antibodies were used and detected by chemiluminescence (Biorad).

Statistical analysis

Statistical analysis was performed using GraphPad Prism 5.0 software (San Diego, CA) and two-way ANOVA test. Data is presented as mean±SEM. Significant differences are indicated with asterisks (* p< 0.05, ** p<0.01, *** p<0.001, ****p<0.0001). For quantitative PCR analysis experiments were repeated at least three times as technical replicates for every sample (different cDNA preparations using the RNA of one liver lobule per mouse) and the average value was calculated. The mean values obtained from individual animals for every group (n=2-3) were used for ANOVA statistical analysis. For quantifications of immunofluorescence signal; for every stained section (representing one mouse liver sample) multiple fields of view were imaged and quantified (see section Microscopy and Image analysis). The average of these values was calculated for every mouse sample. Statistical analyses were performed on the values of all the mouse samples per treatment group (n=2-3 in total).

Cell lines

Activated HSCs (Collagen1alpha1-GFP HSC cell line, David Scholten) and AML12 mouse hepatocytes were used. Cells were serum starved, pretreated with ALK5 inhibitor LY364947 (5ug/ml) for 2 hours and stimulated with TGFβ3 (5ng/ml) for 1, 6 or 20 hours.

Microscopy and Image analysis

Confocal microscopy of labelled specimens was performed on a Leica TC-SP5 microscope with a 40X 1.4 NA oil-immersion objective Z series were collected and reassembled in Image J software (rsbweb.nih.gov/ij). Mean area fraction fluorescence was calculated in Image J software using threshold to select the root boundary and measuring the percentage of positive surface inside the intensity defined by the threshold. For quantifications of immunofluorescence signal, staining experiments were performed on all the samples simultaneously to reduce technical variation (each treatment group contains one sample from each mouse, n=2-3 in total). Experiments were repeated three times (three sections

per sample were analysed) and stained specimens in a given experiment were imaged using identical microscopic exposure and recording settings.

References

1. Serini, G. and G. Gabbiani, Mechanisms of myofibroblast activity and phenotypic modulation. *Exp Cell Res*, 1999. 250(2): p. 273-283.
2. Fausto, N., Liver regeneration and repair: Hepatocytes, progenitor cells, and stem cells. *Hepatology*, 2004. 39(6): p. 1477-1487.
3. Wong, F.W.Y., W.Y. Chan, and S.S.T. Lee, Resistance to carbon tetrachloride-induced hepatotoxicity in mice which lack CYP2E1 expression. *Toxicol Appl Pharmacol*, 1998. 153(1): p. 109-118.
4. Dooley, S. and P. ten Dijke, TGF- β in progression of liver disease. *Cell Tissue Res*, 2012. 347(1): p. 245-256.
5. Michalopoulos, G.K., Liver regeneration. *J Cell Physiol*, 2007. 213(2): p. 286-300.
6. Weber, L.W.D., M. Boll, and A. Stampfl, Hepatotoxicity and mechanism of action of haloalkanes: carbon tetrachloride as a toxicological model. *Crit Rev Toxicol*, 2003. 33(2): p. 105-136.
7. Wells, R.G., The role of matrix stiffness in hepatic stellate cell activation and liver fibrosis. *J Clin Gastroenterol*, 2005. 39(4 Suppl 2): p. S158-61.
8. Böhm, F., et al., Regulation of liver regeneration by growth factors and cytokines. *EMBO Mol Med*, 2010. 2(8): p. 294-305.
9. Braun, L., et al., Transforming growth factor β mRNA increases during liver regeneration: a possible paracrine mechanism of growth regulation. *Proc Natl Acad Sci U S A*, 1988. 85(5): p. 1539-1543.
10. Leask, A., Potential therapeutic targets for cardiac fibrosis: TGF- β , angiotensin, endothelin, CCN2, and PDGF, partners in fibroblast activation. *Circ Res*, 2010. 106(11): p. 1675-1680.
11. Border, W.A. and N.A. Noble, Transforming growth factor β in tissue fibrosis. *N Engl J Med*, 1994. 331(19): p. 1286-1292.
12. Gu, L., et al., Effect of TGF- β /Smad signaling pathway on lung myofibroblast differentiation. *Acta Pharmacol Sin*, 2007. 28(3): p. 382-391.
13. Li, C., L. Suardet, and J.B. Little, Potential role of WAF1/Cip1/p21 as a mediator of TGF- β cytotoxic effect. *J Biol Chem*, 1995. 270(10): p. 4971-4974.
14. Gong, J., et al., Transforming growth factor β 1 increases the stability of p21/WAF1/CIP1 protein and inhibits CDK2 kinase activity in human colon carcinoma FET cells. *Cancer Res*, 2003. 63(12): p. 3340-3346.
15. Hautmann, M.B., C.S. Madsen, and G.K. Owens, A Transforming growth factor β (TGF β) control element drives TGF β -induced stimulation of smooth muscle α -actin gene expression in concert with two CArG elements. *J Biol Chem*, 1997. 272(16): p. 10948-10956.
16. Roy, S.G., Y. Nozaki, and S.H. Phan, Regulation of α -smooth muscle actin gene expression in myofibroblast differentiation from rat lung fibroblasts. *Int J Biochem Cell Biol*, 2001. 33(7): p. 723-734.
17. Heldin, C.H., K. Miyazono, and P. ten Dijke, TGF- β signaling from cell membrane to nucleus through SMAD proteins. *Nature*, 1997. 390(6659): p. 465-471.
18. Heldin, C.H., M. Landström, and A. Moustakas, Mechanism of TGF- β signaling to growth arrest, apoptosis, and epithelial-mesenchymal transition. *Curr Opin Cell Biol*, 2009. 21(2): p. 166-176.
19. Annes, J.P., J.S. Munger, and D.B. Rifkin, Making sense of latent TGF β activation. *J Cell Sci*, 2003. 116(2): p. 217-224.
20. Massagué, J., J. Seoane, and D. Wotton, Smad transcription factors. *Genes Dev*, 2005. 19(23): p. 2783-2810.
21. Yingling, J.M., K.L. Blanchard, and J.S. Sawyer, Development of TGF- β signaling inhibitors for cancer therapy. *Nat Rev Drug Discov*, 2004. 3(12): p. 1011-1022.
22. Flanders, K.C., et al., Mice lacking Smad3 are protected against cutaneous injury induced by ionizing radiation. *Am J Pathol*, 2002. 160(3): p. 1057-1068.
23. Sato, M., et al., Targeted disruption of TGF- β 1/Smad3 signaling protects against renal tubulointerstitial fibrosis induced by unilateral ureteral obstruction. *J Clin Invest*, 2003. 112(10): p. 1486-1494.
24. Jeong, D.H., et al., Smad3 deficiency ameliorates hepatic fibrogenesis through the expression of senescence marker protein-30, an antioxidant-related protein. *Int J Mol Sci*, 2013. 14(12): p. 23700-10.
25. Bhowmick, N.A., et al., TGF- β Signaling in fibroblasts modulates the oncogenic potential of adjacent epithelia. *Science*, 2004. 303(5659): p. 848-851.
26. Pierce, R.A., et al., Increased procollagen mRNA levels in carbon tetrachloride-induced liver fibrosis in rats. *J Biol Chem*, 1987. 262(4): p. 1652-8.

27. Cai, Y., et al, Apoptosis initiated by carbon tetrachloride in mitochondria of rat primary cultured hepatocytes. *Acta Pharmacol Sin*, 2005. 26(8): p. 969-975.
28. Vogt, J., R. Traynor, and G.P. Sapkota, The specificities of small molecule inhibitors of the TGF- β and BMP pathways. *Cell Signal*, 2011. 23(11): p. 1831-1842.
29. Ghavami, S., et al., Apoptosis and cancer: mutations within caspase genes. *J Med Genet*, 2009. 46(8): p. 497-510.
30. Guidotti, J.E., et al., Liver cell polyploidization: a pivotal role for binuclear hepatocytes. *J Biol Chem*, 2003. 278(21): p. 19095-19101.
31. Romero-Gallo, J., et al., Inactivation of TGF- β signaling in hepatocytes results in an increased proliferative response after partial hepatectomy. *Oncogene*, 2005. 24(18): p. 3028-3041.
32. Ghafoory, S., et al., Zonation of nitrogen and glucose metabolism gene expression upon acute liver damage in mouse. *PLoS One*, 2013. 8(10): p. e78262.
33. Tahashi, Y., et al., Differential regulation of TGF- β signal in hepatic stellate cells between acute and chronic rat liver injury. *Hepatology*, 2002. 35(1): p. 49-61.
34. Laping, N.J., et al., Inhibition of Transforming growth factor (TGF)- β 1-induced extracellular matrix with a novel inhibitor of the TGF- β type I receptor kinase activity: SB-431542. *Mol Pharmacol*, 2002. 62(1): p. 58-64.
35. Inman, G.J., et al., SB-431542 is a potent and specific inhibitor of Transforming growth factor- β superfamily type I activin receptor-like kinase (ALK) receptors ALK4, ALK5, and ALK7. *Mol Pharmacol*, 2002. 62(1): p. 65-74.
36. van Beuge, M.M., et al., Enhanced effectivity of an ALK5-inhibitor after cell-specific delivery to hepatic stellate cells in mice with liver injury. *PLoS One*, 2013. 8(2): p. e56442.
37. Yoshioka, N., et al., Small molecule inhibitor of type I transforming growth factor- β receptor kinase ameliorates the inhibitory milieu in injured brain and promotes regeneration of nigrostriatal dopaminergic axons. *J Neurosci Res*, 2011. 89(3): p. 381-393.
38. de Gouville, A.C., et al., Inhibition of TGF- β signaling by an ALK5 inhibitor protects rats from dimethylnitrosamine-induced liver fibrosis. *Br J Pharmacol*, 2005. 145(2): p. 166-177.
39. Petersen, M., et al., Oral administration of GW788388, an inhibitor of TGF- β type I and II receptor kinases, decreases renal fibrosis. *Kidney Int*, 2007. 73(6): p. 705-715.
40. Sorrentino, A., et al., The type I TGF- β receptor engages TRAF6 to activate TAK1 in a receptor kinase-independent manner. *Nat Cell Biol*, 2008. 10(10): p. 1199-1207.
41. Kodama, T., et al., Increases in p53 expression induce CTGF synthesis by mouse and human hepatocytes and result in liver fibrosis in mice. *J Clin Invest*, 2011. 121(8): p. 3343-3356.
42. Manapov, F., P. Muller, and J. Rychly, Translocation of p21Cip1/WAF1 from the nucleus to the cytoplasm correlates with pancreatic myofibroblast to fibroblast cell conversion. *Gut*, 2005. 54(6): p. 814-822.
43. Marhenke, S., et al., p21 promotes sustained liver regeneration and hepatocarcinogenesis in chronic cholestatic liver injury. *Gut*, 2014. 63(9): p. 1501-1512.
44. Wiercinska, E., et al., Id1 is a critical mediator in TGF- β -induced transdifferentiation of rat hepatic stellate cells. *Hepatology*, 2006. 43(5): p. 1032-1041.
45. Sato, Y., et al., Resolution of liver cirrhosis using vitamin A-coupled liposomes to deliver siRNA against a collagen-specific chaperone. *Nat Biotech*, 2008. 26(4): p. 431-442.
46. Chu, W., et al., Arsenic-induced interstitial myocardial fibrosis reveals a new insight into drug-induced long QT syndrome. *Cardiovasc Res*, 2012. 96(1): p. 90-98.
47. Oka, M., et al., Inhibition of endogenous TGF- β signaling enhances lymphangiogenesis. *Blood*, 2008. 111(9): p. 4571-9.
48. Naka, K., et al., TGF- β -FOXO signaling maintains leukaemia-initiating cells in chronic myeloid leukaemia. *Nature*, 2010. 463(7281): p. 676-680.

